

Set-Based Computation of Vehicle Behaviors for the Online Verification of Autonomous Vehicles

Matthias Althoff and John M. Dolan

Abstract—We compute the set of all possible behaviors of an autonomous vehicle using reachability analysis. A reachable set is the set of states a system can reach for a given set of initial states, disturbances, and sensor noise values. We consider autonomous vehicles which plan trajectories for a certain look-ahead horizon which are followed using feedback control. While a perfectly followed trajectory might not violate specified safety properties (e.g. lane departures or vehicle collisions), a violating deviation from the planned trajectory might exist. Given the mathematical model of the controlled vehicle and bounds on uncertainty, our approach detects any possible violation. In addition, the approach provides results faster than the time required to finish the planned maneuvers of the autonomous vehicle.

I. INTRODUCTION

One of the main motivations for the development of (semi-)autonomous vehicles is to prevent accidents caused by human error. Compared to humans, a computer-controlled vehicle can predict its future behavior more precisely when a mathematical description of the vehicle and its maneuver is provided. Based on these predictions, one can compute if the vehicle stays within lane boundaries and if static as well as dynamic obstacles are avoided. However, in reality, the exact behavior cannot be predicted due to uncertainties in the initial state, sensor measurements, and vehicle models. A commonly used technique to cope with those uncertainties is to compute many simulations. The drawback is that the number of required simulation runs typically scales exponentially with the number of uncertain variables in order to achieve a certain coverage of possible behaviors. This dilemma can be overcome by computing reachable sets which enclose all possible simulations of a system (full coverage). In this work, an approach is presented to compute the reachable set of an autonomous vehicle faster than the execution time of the actual maneuver.

There is a rich literature on reachability analysis of dynamical systems with continuous or hybrid (mixed discrete/continuous) dynamics. Many of the recent advances are summarized in [1] and the references therein. Since the vehicle model in this paper has nonlinear continuous dynamics, we focus on this class of systems: Most approaches compute reachable sets of nonlinear systems by abstracting to differential inclusions of simpler dynamics. Earlier approaches simplify the dynamics within regions of

a fixed state space partition [2], [3], which generally causes an exponential growth in required regions with respect to the number of state variables. To overcome this problem, more recent work computes abstractions in the vicinity of the reachable set [4]–[6]. Approaches which do not use abstraction are mostly based on optimization techniques which are computationally expensive [7]. The method applied in this work is based on [5], which uses zonotopes as a set representation for nonlinear systems in contrast to the other referenced approaches. As a consequence, the proposed approach, which abstracts to linear systems, is efficient, since zonotopes show great performance for linear systems [8].

The literature on reachability analysis applied to autonomous vehicles and car-like robots is rather limited. Unlike the current work, most previous work considers simple dynamic models. A frequently used model is to bound the acceleration in the 2-dimensional plane such that the set of positions are circles when the initial set is a circle [9], [10]. Reachability analysis of slightly more complex models has been performed in coverage and pursuer problems using a non-holonomic Dubins vehicle [11], a tricycle model [12], or vehicles in environments dominated by external drift [13].

There is more work on verifying maneuvers for the related problem of aircraft safety by computing reachable sets based on Hamilton-Jacobi partial differential equations, see e.g. [14], [15]. Unlike in the current work, the considered flight maneuvers are verified offline.

Besides reachability analysis, there is also work on verification of road traffic using theorem proving [16], which is less adequate for online applications since user interaction is typically required.

Online verification of road traffic scenes using reachability analysis has been presented in an earlier work for vehicles tracking arc segments at constant velocity, yielding linear system dynamics [17]. This work is an extension in many respects. First, the planned trajectory can be arbitrary instead of being restricted by connected arc segments. Second, the velocity of the maneuvers varies over time instead of being constant. Due to these two generalizations the differential equations describing the vehicle dynamics are no longer linear, but nonlinear, which makes reachability analysis much harder. Third, we consider measurement uncertainties which have not been considered in the previous work, and fourth, we make suggestions for parallelizing the computations.

II. VERIFICATION CONCEPT

In this work, we present a technique to compute all possible behaviors of an autonomous vehicle under uncertain

Matthias Althoff is with Faculty of Electrical and Computer Engineering, Carnegie Mellon University, Pittsburgh, PA 15213, USA, email: malthoff@ece.cmu.edu

John Dolan is with the Robotics Institute, Carnegie Mellon University, Pittsburgh, PA 15213, USA, email: jmd@cs.cmu.edu

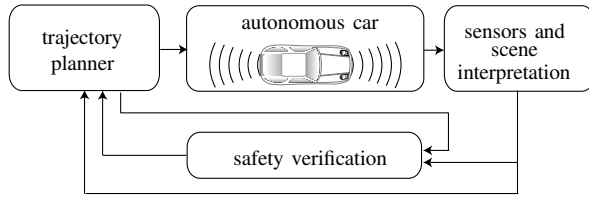


Fig. 1. Concept of the safety verification.

measurements and initial states. One of the main applications of this method is a safety verification module for autonomous vehicles which decides if a maneuver can be safely executed, see Fig. 1. The maneuvers are mathematically described by reference trajectories which are functions over time, describing the goal position on the road. Trajectory tracking is performed by a feedback controller which will be described later in more detail.

The safety verification module requires information on the road network, as well as on static and dynamic obstacles for collision checks. The trajectory to be checked is provided from a trajectory planner. We assume that the suggested trajectories already passed a collision check under the assumption that the vehicle perfectly follows the trajectory. This reduces the number of trajectories that have to be checked by more costly reachable set computations.

Depending on the reference trajectory to be checked, the verification is for finite or infinite time. The infinite verification can be achieved by additionally planning a braking maneuver which brings the vehicle to a safe stop – a condition in which the vehicle can stay forever without causing a crash. A stop is not considered safe if the vehicle stops in an intersection, a railroad crossing, or other unsafe locations. Note that the vehicle only executes the beginning of the reference trajectory while it is continuously replanned and verified such that the stops are not necessarily executed unless no safe alternative maneuver is to be found.

III. MODEL OF THE CONTROLLED VEHICLE

In order to compute the reachable set of the autonomous car, a mathematical model is required. We first derive the dynamics of the vehicle and secondly introduce a controller for trajectory tracking. The combination of both models yields the overall system dynamics for the subsequently described reachability analysis. Note that the presented technique also works for different vehicle models which do not have to be controlled. However, uncontrolled vehicles typically have a larger reachable set which might require splitting of reachable sets to properly handle linearization errors [5].

A. Vehicle Model

The vehicle model is an extended bicycle model which consists of 6 states: the slip angle at the center of mass $x_1 = \beta$, the heading angle $x_2 = \Psi$, the yaw rate $x_3 = \dot{\Psi}$, the velocity $x_4 = v$, the x-position $x_5 = s_x$, and the y-position $x_6 = s_y$, see Fig. 2. The bicycle model is widely used for control designs involving lateral vehicle dynamics and its

name refers to the fact that the front and rear wheel pairs are each lumped into one wheel, since the roll dynamics is not considered [18, Chap. 2.6]. The bicycle model is accurate for small longitudinal accelerations and a tire model which linearly relates lateral force and slip angle. However, tires saturate at large slip angles, which is considered unsafe, so that reference trajectories causing tire saturation are returned as unsafe and are not further verified. For large longitudinal accelerations, the vertical force shifts between the front and rear axle, which is not yet considered. Although this effect is not dominant, we plan to consider it in future work.

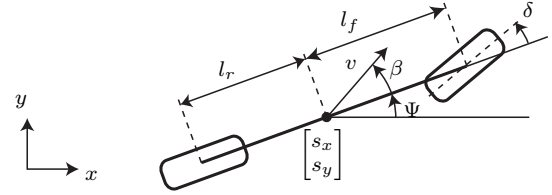


Fig. 2. Bicycle model.

The differential equations of the vehicle dynamics are given in (1), where the equations for \dot{x}_1 and \dot{x}_3 describe the yaw dynamics of the bicycle model, where C_f and C_r are the front and rear cornering stiffness. The heading angle x_2 is obtained by integration of the yaw rate x_3 and the velocity x_4 by integration of the longitudinal acceleration a_x , see (1). Finally, the velocity and the direction of the center of mass ($x_1 + x_2$) are used to geometrically obtain the position coordinates x_5 and x_6 .

$$\begin{aligned}
 \dot{x}_1 &= \left(\frac{C_r l_r - C_f l_f}{m x_4^2} - 1 \right) x_3 + \frac{1}{m x_4} (C_f \delta - (C_f + C_r) x_1) \\
 \dot{x}_2 &= x_3 \\
 \dot{x}_3 &= \frac{1}{I_z} \left((l_r C_r - l_f C_f) x_1 - (l_f^2 C_f + l_r^2 C_r) \frac{x_3}{x_4} + l_f C_f \delta \right) \\
 \dot{x}_4 &= a_x \\
 \dot{x}_5 &= x_4 \cos(x_1 + x_2) \\
 \dot{x}_6 &= x_4 \sin(x_1 + x_2)
 \end{aligned} \tag{1}$$

B. Tracking Controller

In this subsection, the controllers for the steering angle δ and the acceleration command a_x are designed. It is assumed that the vehicle has internal controls which make it possible to realize commanded steering angles and acceleration commands at high accuracy. Uncertainties due to unmodeled dynamics of internal controllers can be considered by enlarging the set of uncertain inputs.

The task of the tracking controller is to follow a reference trajectory which is specified at discrete points in time $t_k = k r$, where $k \in \mathbb{N}$ is the time step and $r \in \mathbb{R}^+$ is the step size. The values of the reference trajectory are constant in between, i.e., during the time intervals $[t_k, t_{k+1}]$. For compactness we introduce the time interval $\tau_k := [t_k, t_{k+1}]$. The reference trajectory consists of the desired values of the

x- and y-position $s_{x,d}$, $s_{y,d}$ in a global coordinate system, from which the desired yaw angle Ψ_d , yaw rate $\dot{\Psi}_d$ and velocity v_d can be derived.

For the lateral and longitudinal control we use the position deviations ϵ_x and ϵ_y in the local coordinates of the reference trajectory (see Fig. 3):

$$\begin{aligned}\epsilon_x &= \cos(\Psi_d)(s_{x,d} - s_x) + \sin(\Psi_d)(s_{y,d} - s_y), \\ \epsilon_y &= -\sin(\Psi_d)(s_{x,d} - s_x) + \cos(\Psi_d)(s_{y,d} - s_y).\end{aligned}$$

For the lateral control we use the lateral deviation ϵ_y , as well as the deviations from the yaw angle and yaw rate, to stabilize ϵ_y around zero:

$$\delta = k_1\epsilon_y + k_2(\Psi_d - \Psi) + k_3(\dot{\Psi}_d - \dot{\Psi}).$$

For the longitudinal control we use the longitudinal deviation ϵ_x and the velocity deviation $\epsilon_v(t) = v_d(t) - v(t)$:

$$a_x = k_4\epsilon_x + k_5\epsilon_v.$$

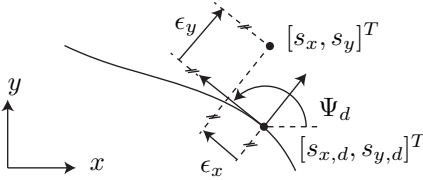


Fig. 3. Trajectory tracking: auxiliary variables.

It remains to introduce sensor noise in order to study the controller performance in realistic conditions. We use a positioning system that combines GPS data with inertial measurements to accurately measure the positions s_x , s_y , the yaw angle Ψ , the yaw rate $\dot{\Psi}$, and the velocity v . The corresponding sensor noise is denoted by u_x , u_y , u_Ψ , $u_{\dot{\Psi}}$, and u_v . After introducing the sensor noise vector $u = [u_x, u_y, u_\Psi, u_{\dot{\Psi}}, u_v]^T$ and the reference vector $w = [s_{x,d}, s_{y,d}, \Psi_d, \dot{\Psi}_d, v_d]^T$, the final control equations are

$$\begin{aligned}\delta &= k_1 \left(\cos(w_3)(w_2 - x_6 - u_2) - \sin(w_3)(w_1 - x_5 - u_1) \right) \\ &\quad + k_2(w_3 - x_2 - u_3) + k_3(w_4 - x_3 - u_4), \\ a_x &= k_4 \left(\cos(w_3)(w_1 - x_5 - u_1) + \sin(w_3)(w_2 - x_6 - u_2) \right) \\ &\quad + k_5(w_5 - x_4 - u_5).\end{aligned}$$

Inserting the above equations $\delta = f_\delta(x, w, u)$ and $a_x = f_{a_x}(x, w, u)$ into (1) results in the final differential equation of the controlled vehicle $\dot{x} = f(x, w, u)$ which is used for reachability analysis.

IV. REACHABILITY ANALYSIS

This section summarizes the steps necessary to compute the set of states the controlled vehicle with the dynamics $\dot{x} = f(x, w, u)$ can reach. Besides uncertain initial states $x(0) \in \mathcal{R}(0)$, we will also allow uncertain sensor noise values $u(t) \in \mathcal{U}$, where the only requirement for $u(t)$ is that it is piecewise-continuous so that a solution $x(t)$ is guaranteed. Thus, we capture arbitrary noise frequencies of $u(t)$.

We denote the solution to $\dot{x} = f(x, w, u)$ for $x(0) = x_0$, $t \in [0, t_f]$, and trajectories $w(\cdot)$, $u(\cdot)$ by $\chi(t, x_0, w(\cdot), u(\cdot))$. Note that $w(\cdot)$ refers to a trajectory, where $w(t)$ refers to the value of the trajectory at time t . The exact reachable set for a given reference trajectory $w^*(\cdot)$ and a set of sensor noise values \mathcal{U} is

$$\begin{aligned}\mathcal{R}^e([0, t_f]) &= \left\{ \chi(t, x_0, w(\cdot), u(\cdot)) \mid x_0 \in \mathcal{R}(0), t \in [0, t_f], \right. \\ &\quad \left. w(t) = w^*(t), u(t) \in \mathcal{U} \right\}.\end{aligned}$$

In general, the set of reachable states cannot be computed exactly [19], so that one has to compute overapproximations defined as $\mathcal{R}([0, t_f]) \supseteq \mathcal{R}^e([0, t_f])$. In this work, the reachable set of the time interval $[0, t_f]$ is obtained by computing reachable sets of smaller time intervals $\tau_k = [t_k, t_{k+1}]$, where t_k equals the times at which the reference vector $w(t_k)$ is updated, see Sec. III-B. It would also be possible to choose fractions of τ_k as time intervals for the reachable set computation. The final reachable set is represented by a list of sets for all time intervals.

The overapproximations in this work are obtained by linearizing the nonlinear dynamics $\dot{x} = f(x, w, u)$ so that techniques for linear systems can be applied as proposed in an earlier work [5]. In order to guarantee an overapproximative result, the linearization error is considered as an additional uncertain input, as presented in the next subsection.

A. Conservative Linearization

For a concise notation of the linearization procedure, the state vector x and the input vector u are combined in a new vector $z = [x^T, u^T]^T$. The reference trajectory is not included, since it is certain, and thus a linearization with respect to that vector is not required. Using a first-order Taylor expansion around the linearization point $[z^{*T}, w^{*T}]^T$, the original differential equation of the i^{th} coordinate is enclosed by the differential inclusion

$$\begin{aligned}\forall t \in \tau_k : \\ \dot{x}_i \in f_i(z^*, w^*) + \underbrace{\frac{\partial f_i(z, w^*)}{\partial z} \Big|_{z=z^*} (z - z^*)}_{=[A(x-x^*)+B(u-u^*)]_i} \oplus \mathcal{L}_i(\tau_k),\end{aligned}$$

where \oplus denotes a Minkowski addition¹ and \mathcal{L} is the set of Lagrange remainders

$$\mathcal{L}_i(\tau_k) = \left\{ \frac{1}{2} (z - z^*)^T \frac{\partial^2 f_i(\xi, w^*)}{\partial z^2} (z - z^*) \mid \xi \in \mathcal{R}(\tau_k) \times \mathcal{U} \right\}$$

The Lagrange remainder covers all possible linearization errors when ξ may vary arbitrarily in the set of possible values of x and u given by the Cartesian product $\mathcal{R}(\tau_k) \times \mathcal{U}$, see [20].

The linearization point is updated for each time interval τ_k . A good linearization point is $z^*(\tau_k) = \text{center}(\mathcal{R}(\tau_k) \times \mathcal{U})$ (see [5]), where $\text{center}()$ returns the volumetric center of a set. Since the reachable sets $\mathcal{R}(\tau_k)$ are not known in advance, the vector $x^*(\tau_k)$ of z^* is chosen as the state values $x(t_k)$

¹Given are sets in Euclidean space \mathcal{A}, \mathcal{B} : $\mathcal{A} \oplus \mathcal{B} = \{a+b \mid a \in \mathcal{A}, b \in \mathcal{B}\}$

of a nominal trajectory obtained by a simulation starting in the center of $\mathcal{R}(0)$ under the input $u(t) = \text{center}(\mathcal{U})$.

Given the linearization points for each time interval, the conservative linearization is obtained as follows:

- 1) Define a set of allowed linearization errors $\bar{\mathcal{L}}(\tau_k)$ which should be a superset of the exact set of linearization errors.
- 2) Compute the reachable set $\bar{\mathcal{R}}(\tau_k)$ of the linearized system $\dot{x} \in f(z^*, w^*) + A(x - x^*) + B(u - u^*) \oplus \bar{\mathcal{L}}(\tau_k)$ as shown in the next subsection.
- 3) Compute the linearization errors $\mathcal{L}(\tau_k)$ based on $\bar{\mathcal{R}}(\tau_k)$ according to [5].
- 4) Check if $\mathcal{L}(\tau_k) \subseteq \bar{\mathcal{L}}(\tau_k)$, otherwise abort and return unsafe.
- 5) Compute the refined set $\mathcal{R}(\tau_k)$ as in step 2 using \mathcal{L} instead of $\bar{\mathcal{L}}$.
- 6) Repeat this procedure for further time intervals.

Alternatively, step 4 can be replaced by a procedure for $\mathcal{L}(\tau_k) \not\subseteq \bar{\mathcal{L}}(\tau_k)$ which splits the reachable set so that $\mathcal{L}(\tau_k)$ becomes smaller and the computation can be continued, see [5]. The procedure for computing reachable sets of linear systems is described in the next subsection.

B. Reachable Set Computation of Linear Systems

The reachable set computation for linear systems takes advantage of the superposition principle, allowing one to separately obtain the reachable set due to the initial state solution and the input solution, denoted by \mathcal{R}^h and \mathcal{R}^i , respectively. The step-by-step computation is illustrated in Fig. 4:

- 1) Compute the exact set of initial state solutions as $\mathcal{R}^h(t_{k+1}) = e^{Ar}\mathcal{R}(t_k)$.
- 2) Compute the convex hull $\mathcal{R}_{\text{CH}}^h(\tau_k)$ of $\mathcal{R}(t_k)$ and $\mathcal{R}^h(t_{k+1})$ which encloses all trajectories for $t \in \tau_k = [t_k, t_{k+1}]$ under the assumption that trajectories within the time interval are straight lines.
- 3) Enlarge the convex hull by the set product² $\mathcal{F}(t_k) \otimes \mathcal{R}(t_k)$ to consider the curvature of trajectories, and by $\mathcal{R}^i(\tau_k)$ to consider uncertain inputs. A detailed description for computing \mathcal{F} and \mathcal{R}^i can be found in [21], where \mathcal{F} is an interval matrix. Thus, the reachable set is obtained as $\mathcal{R}(\tau_k) = \mathcal{R}_{\text{CH}}^h(\tau_k) \oplus (\mathcal{F}(t_k) \otimes \mathcal{R}(t_k)) \oplus \mathcal{R}^i(\tau_k)$.

Besides the time interval solution $\mathcal{R}(\tau_k)$, the set $\mathcal{R}(t_{k+1}) = \mathcal{R}^h(t_{k+1}) \oplus \mathcal{R}^i(t_{k+1})$ has to be computed, since the algorithm starts with the set at fixed times t_k , see step 1.

The Minkowski addition of $\mathcal{R}^h(t_{k+1})$ and $\mathcal{R}^i(t_{k+1})$ increases the representation order of the reachable set, which requires reduction methods causing the so-called wrapping-effect due to the propagation of overapproximations through successive time steps. In this work, reachable sets are represented by zonotopes, for which efficient reduction techniques exist [22], [23].

²Given are sets in Euclidean space \mathcal{A}, \mathcal{B} : $\mathcal{A} \otimes \mathcal{B} = \{ab | a \in \mathcal{A}, b \in \mathcal{B}\}$

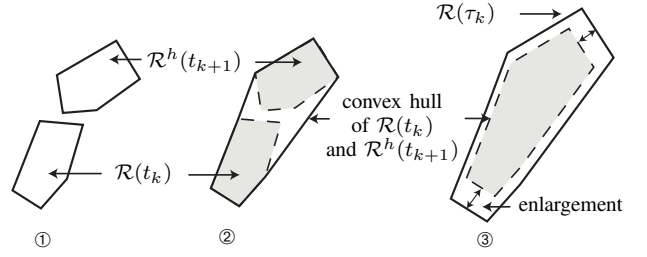


Fig. 4. Computation of the reachable set for a time interval.

V. SET OF OCCUPIED POSITIONS

The ultimate goal of the reachability analysis is to check if the vehicle stays on the road and if a crash is possible, which requires knowing the occupancy of the vehicle body on the road. The relevant variables from the reachability computation to determine the occupancy on the road are the x- and y-position (s_x, s_y) and the orientation Ψ . We denote the projections of the reachable set onto the position coordinates as \mathcal{R}_s (2-dimensional) and onto the orientation as \mathcal{R}_Ψ (1-dimensional).

We model the vehicle body as a rectangle with width b_w and length b_l . For each time interval τ_k , the rectangle is oriented according to the center of possible orientations $\Psi_c = \text{center}(\mathcal{R}_\Psi)$. The deviation around this center $\Delta\Psi = \max_{\Psi^* \in \mathcal{R}_\Psi} (|\Psi^* - \Psi_c|) \geq 0$ is considered by enlarging the vehicle body as illustrated in Fig. 5, where

$$\begin{aligned} \Delta b_{l,\Psi} &= |(1 - \cos(\Delta\Psi))b_l - \sin(\Delta\Psi)b_w|, \\ \Delta b_{w,\Psi} &= |(1 - \cos(\Delta\Psi))b_w - \sin(\Delta\Psi)b_l|. \end{aligned}$$

The uncertain position of the center of mass is also considered by enlarging the body size, while the center of the vehicle body is shifted to $\text{center}(\mathcal{R}_s)$. The enlargement due to uncertain positions can be obtained by rotating the set of positions by $-\Psi_c$ and computing an enclosing interval for each dimension. The box enclosure operation $\text{box}()$ can be efficiently done for zonotopes, which are used for reachable set computations.

$$\begin{aligned} \left(\begin{array}{c} [-\Delta b_{l,s}, \Delta b_{l,s}] \\ [-\Delta b_{w,s}, \Delta b_{w,s}] \end{array} \right) &= \text{box}(T(\mathcal{R}_s - \text{center}(\mathcal{R}_s))), \\ T &= \begin{pmatrix} \cos(-\Psi_c) & -\sin(-\Psi_c) \\ \sin(-\Psi_c) & \cos(-\Psi_c) \end{pmatrix}. \end{aligned}$$

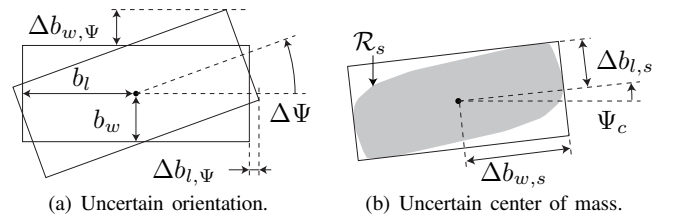


Fig. 5. Enlargement of the vehicle occupation due to uncertain orientation and position.

Once the set of possible occupation is obtained, one has to check if collisions with other vehicles or road boundaries exist. In this work, the occupation at time intervals is

overapproximated by axis-aligned boxes, and only if axis-aligned boxes intersect is the more elaborate collision check of oriented boxes computed [17]. Another method is to inscribe the occupied sets by several circles [24].

VI. NUMERICAL EXAMPLE

In this section we illustrate the usefulness of the reachable set computations for the online verification of traffic scenes. Note that the reachability results can also be used to evaluate the performance of controllers under sensor noise and uncertain initial states.

The considered scenario presents an evasive maneuver of the autonomous car caused by a pedestrian who steps into the road without respecting oncoming traffic. In addition, the autonomous car has to avoid a collision with an oncoming car while respecting the road limits. The first part of the maneuver is a combined braking and steering maneuver with lateral acceleration of $\pm 0.8g$ and longitudinal acceleration of $-0.2g$, where g is the gravity constant. This part of the maneuver is almost at the limit of maximum possible tire force, whereas the second part induces smaller acceleration values, since it is only required to steer back into the original lane before hitting oncoming traffic.

The vehicle, sensor, and control parameters of the numerical example are listed in Tab. I. The vehicle parameters are taken from a 1986 Pontiac 6000 STE sedan [25] and the standard deviations σ of the sensor noise for u_x , u_y , and u_ψ are taken from the Applanix POS LV platform, whose specifications can be found online. The standard deviation for the other noise sources are reasonably chosen. The interval of possible sensor noises is chosen as the 4σ interval, which corresponds to a probability of 0.99994 that the sensor noise is in the interval when it is assumed to be Gaussian. The set of initial states for the considered maneuver is $\mathcal{R}(0) = [-0.02, 0.02] \text{ rad} \times [-0.05, 0.05] \text{ rad} \times [-0.3, 0.1] \text{ rad/s} \times [14.8, 15.2] \text{ m/s} \times [-0.2, 0.2] \text{ m} \times [-0.5, -0.1] \text{ m}$. The body size of the autonomous car is $b_l = 4.5 \text{ m}$, $b_w = 1.8 \text{ m}$ and the time step for updating the reference trajectory is $r = 0.01 \text{ s}$, which is also the step size of the reachable set computation.

TABLE I
VEHICLE PARAMETERS.

vehicle parameters				
m	I_z	$C_f = C_r$	l_f	l_r
1573 kg	2873 kg m ²	8e4 N/rad	1.1 m	1.58 m
sensor noise intervals, $\rho = [-1, 1]$				
u_x	u_y	u_ψ	$u_{\dot{\psi}}$	u_v
$0.08\rho \text{ m}$	$0.08\rho \text{ m}$	$\frac{0.2\pi}{180}\rho \text{ rad}$	$\frac{0.2\pi}{180}\rho \text{ rad/s}$	$0.08\rho \text{ m/s}$
control parameters				
k_1	k_2	k_3	k_4	k_5
1	10	2	1	10

The reachable sets for different projections are shown in Fig. 6. It can be seen that random simulations are enclosed by the reachable set. The simulations indicate that the overapproximation of the position deviation (s_x, s_y) as well as the other coordinates is small. In Fig. 7, the occupancy

of the autonomous car and the oncoming car are shown. For the oncoming car it is assumed that the maximum speed is 20% higher than the speed limit of 15 m/s, the acceleration interval is $[-0.7, 0.7] \text{ g}$, and the vehicle does not drive backwards. The initial longitudinal position and velocity are $[110, 120] \text{ m}$ and $[13, 15] \text{ m/s}$. It is assumed that the other vehicle only uses its own lane, but possibly occupies the full width of the lane. Due to braking, the vehicle may stop at 108 m (see stopping line in Fig. 7). It can be concluded that the autonomous car stays within the road width limits from -1.75 m to 5.25 m (lane width 3.5 m) and avoids a crash with the oncoming vehicle.

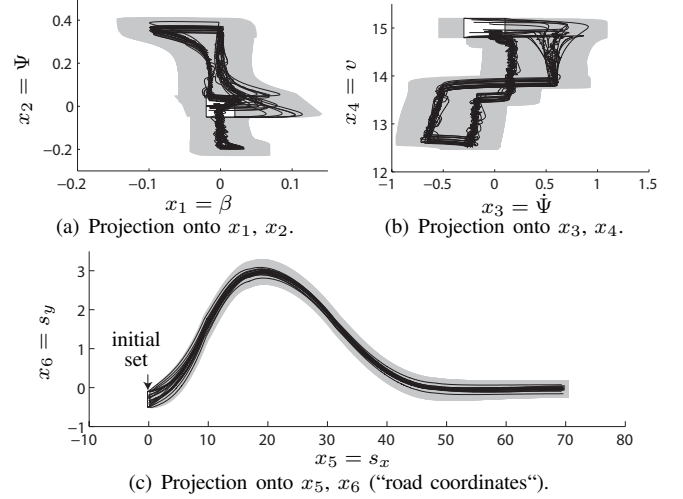


Fig. 6. Reachable set for the evasive maneuver. The white set shows the set of initial states, black lines show random simulation results.

All computations have been performed on an Intel i7 Processor with 1.6 GHz and 6 GB memory in MATLAB. The reachable set computation can be separated into 4 processes: The first one, called process A, linearizes the system dynamics along the nominal trajectory described in Sec. IV-A. This process also performs parallel computation of $e^{A(\tau_k)r}$, $\mathcal{F}(t_k)$, and $\mathcal{R}^i(\tau_k)$ (only for the assumed linearization errors), which took 1.56 s using 4 cores. The reachable set computations which cannot be parallelized are computed by process B in 2.24 s. A significant time reduction for process B could be achieved by replacing interval arithmetic for computing the linearization errors \mathcal{L} by evaluating corner cases due to the monotonicity properties of the specific Lagrange remainder herein (see [26]). The computation for transforming the reachable set to the occupancy of the vehicle (process C) took 0.46 s and the collision check took 0.25 s (process D). For the reachable set computation of each time interval, process A (pre-processing), and processes C, D (post-processing) are faster than process B, so that all processes can be run in parallel and process B determines the overall computation time of 2.24 s. Considering that the maneuver took 5 s, the current implementation is about 2 times faster than the execution time of the maneuver. By implementing the algorithm in C++ on a real vehicle, it is expected that the efficiency will be significantly improved. This improvement

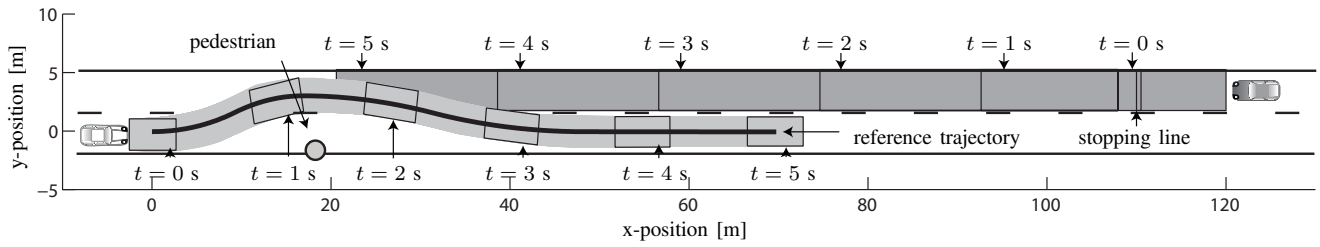


Fig. 7. Occupancy set for the evasive maneuver. The gray regions show the occupancies of the autonomous and the other car, the black line shows the path the autonomous car should follow. The occupancy at selected times is indicated by black boxes.

is especially required in unexpected situation changes such as the pedestrian stepping into the road in the discussed example, for which a verification should be done faster than the reaction time of a human driver (≈ 0.3 s).

VII. CONCLUSIONS AND FUTURE WORK

We have presented an algorithm that can predict all possible behaviors of an autonomous car given a dynamic model, a set of initial states, and bounds on sensor noise. The set of all possible trajectories of a vehicle makes it possible to detect crashes in traffic scenes. It has been demonstrated that the approach can be computed faster than the execution time of the maneuver, and further improvements can be expected by implementing the algorithms in C++. Other future work involves considering uncertain vehicle parameters, such as the tire-road friction coefficient, or the weight distribution due to loading the trunk or longitudinal accelerations.

ACKNOWLEDGEMENTS

The authors gratefully acknowledge partial financial support by the NSF Cyberphysical Systems Program, Award CNS1035813, and by the NSF Expeditions in Computing Program, Award CCF0926181.

REFERENCES

- [1] E. Asarin, T. Dang, G. Frehse, A. Girard, C. Le Guernic, and O. Maler, "Recent progress in continuous and hybrid reachability analysis," in *Proc. of the 2006 IEEE Conference on Computer Aided Control Systems Design*, 2006, pp. 1582–1587.
- [2] A. Puri, P. Varaiya, and V. Borkar, " ϵ -approximation of differential inclusions," in *Proc. of the 34th IEEE Conference on Decision and Control*, 1995, pp. 2892 – 2897.
- [3] E. Asarin, T. Dang, and A. Girard, "Reachability analysis of nonlinear systems using conservative approximation," in *Hybrid Systems: Control and Computation*, 2003, pp. 20–35.
- [4] Z. Han and B. H. Krogh, "Reachability analysis of nonlinear systems using trajectory piecewise linearized models," in *Proc. of the American Control Conference*, 2006, pp. 1505–1510.
- [5] M. Althoff, O. Stursberg, and M. Buss, "Reachability analysis of nonlinear systems with uncertain parameters using conservative linearization," in *Proc. of the 47th IEEE Conference on Decision and Control*, 2008, pp. 4042–4048.
- [6] T. Dang, O. Maler, and R. Testylier, "Accurate hybridization of nonlinear systems," in *Hybrid Systems: Computation and Control*, 2010, pp. 11–19.
- [7] A. Chutinan and B. H. Krogh, "Computational techniques for hybrid system verification," *IEEE Transactions on Automatic Control*, vol. 48, no. 1, pp. 64–75, 2003.
- [8] A. Girard, C. Le Guernic, and O. Maler, "Efficient computation of reachable sets of linear time-invariant systems with inputs," in *Hybrid Systems: Computation and Control*, ser. LNCS 3927. Springer, 2006, pp. 257–271.
- [9] C. Schmidt, F. Oechsle, and W. Branz, "Research on trajectory planning in emergency situations with multiple objects," in *Proc. of the IEEE Intelligent Transportation Systems Conference*, 2006, pp. 988–992.
- [10] J. van den Berg, "Path planning in dynamic environments," Ph.D. dissertation, Utrecht University, 2007.
- [11] K. Savla, F. Bullo, and E. Frazzoli, "The coverage problem for loitering Dubins vehicles," in *Proc. of the 46th IEEE Conference on Decision and Control*, 2007, pp. 1398–1403.
- [12] C. F. Chung, T. Furukawa, and A. H. Göktozan, "Coordinated control for capturing a highly maneuverable evader using forward reachable sets," in *Proc. of the IEEE International Conference on Robotics and Automation*, 2006, pp. 1336–1341.
- [13] A. Kwok and S. Martínez, "A coverage algorithm for drifters in a river environment," in *Proc. of the American Control Conference*, 2010, pp. 6436–6441.
- [14] C. Tomlin, I. Mitchell, and R. Ghosh, "Safety verification of conflict resolution maneuvers," *IEEE Transactions on Intelligent Transportation Systems*, vol. 2, pp. 110–120, 2001.
- [15] J. H. Gillula, H. Haomiao, M. P. Vitus, and C. J. Tomlin, "Design of guaranteed safe maneuvers using reachable sets: Autonomous quadrotor aerobatics in theory and practice," in *Proc. of the IEEE International Conference on Robotics and Automation*, 2010, pp. 1649–1654.
- [16] S. M. Loos, A. Platzer, and L. Nistor, "Adaptive cruise control: Hybrid, distributed, and now formally verified," in *Proc. of the 17th International Symposium on Formal Methods*, ser. LNCS 6664. Springer, 2011, pp. 42–56.
- [17] M. Althoff, D. Althoff, D. Wollherr, and M. Buss, "Safety verification of autonomous vehicles for coordinated evasive maneuvers," in *Proc. of the IEEE Intelligent Vehicles Symposium*, 2010.
- [18] R. Rajamani, *Vehicle Dynamics and Control*, F. F. Ling and E. F. Gloyna, Eds. Springer, 2006.
- [19] G. Lafferriere, G. J. Pappas, and S. Yovine, "Symbolic reachability computation for families of linear vector fields," *Symbolic Computation*, vol. 32, pp. 231–253, 2001.
- [20] M. Berz and G. Hoffstätter, "Computation and application of Taylor polynomials with interval remainder bounds," *Reliable Computing*, vol. 4, pp. 83–97, 1998.
- [21] M. Althoff, "Reachability analysis and its application to the safety assessment of autonomous cars," Dissertation, TU München, 2010, URL: <http://nbn-resolving.de/urn/resolver.pl?urn:nbn:de:bvb:91-diss-20100715-963752-1-4>.
- [22] W. Kühn, "Rigorously computed orbits of dynamical systems without the wrapping effect," *Computing*, vol. 61, pp. 47–67, 1998.
- [23] A. Girard, "Reachability of uncertain linear systems using zonotopes," in *Hybrid Systems: Computation and Control*, ser. LNCS 3414. Springer, 2005, pp. 291–305.
- [24] J. Ziegler and C. Stiller, "Fast collision checking for intelligent vehicle motion planning," in *Proc. of the IEEE Intelligent Vehicles Symposium*, 2010, pp. 518–522.
- [25] J. Guldner, W. Sienel, H.-S. Tan, J. Ackermann, S. Patwardhan, and T. Bünte, "Robust automatic steering control for look-down reference systems with front and rear sensors," *IEEE Transactions on Control Systems Technology*, vol. 7, pp. 2–11, 1999.
- [26] N. Ramdani, N. Meslem, and Y. Candau, "Computing reachable sets for uncertain nonlinear monotone systems," *Nonlinear Analysis: Hybrid Systems*, vol. 4, pp. 263–278, 2010.